

MINERALOGICAL CHARACTERISATION TECHNIQUES FOR PREDICTING ACID ROCK DRAINAGE

Anita Parbhakar

CODES ARC Centre of Excellence in Ore Deposits, University of Tasmania, Australia

Mansour Edraki

Centre of Mined Land Rehabilitation, Sustainable Minerals Institute, University of Queensland, Australia

Dee Bradshaw and Stephen Walters

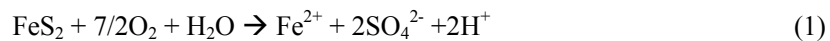
Julius Kruttschnitt Mineral Research Centre, Sustainable Minerals Institute, University of Queensland, Australia

ABSTRACT

Fifty-one waste rock samples collected from an abandoned mine in north Queensland, Australia were characterised by routine and advanced geochemical tests to aid the development of a mineralogical Acid Rock Drainage (ARD) Index. The ARD Index comprises five categories (diameter/size, degree of alteration and morphology of acid generating phase; content of neutralising phases and spatial relationship between acid generating and neutralising phases). Polished rock slices (up to 5cm diameter) and petrographic thin sections were evaluated by these criteria and scored out of 50, with a higher number representing a greater acid generating potential. Ten mesotextural groups were identified and extensive geochemical testing confirmed there to be four potentially acid forming mesotextures (C, G, H & J). Classification using the mineralogical ARD Index recognised only two mesotextures as significantly acid forming (mesotextures H & J). ARD Index values were cross-checked against paste pH values which confirmed mesotextures C and G as not acid forming which is in agreement with the sulphide mineralogy. This demonstrates that static geochemical testing has overestimated acid generating potential. Ongoing work is focused on developing ARD predictive protocols using automated mineralogical platforms such as Mineral-Liberation-Analyser-Scanning Electron Microscopy (MLA-SEM) and micro-X-Ray Fluorescence (μ -XRF) to identify potentially acid generating textures and to predict deleterious element issues.

INTRODUCTION & BACKGROUND

In mine waste materials containing iron-sulphide minerals such as pyrite and pyrrhotite, acid rock drainage (ARD) can be produced due to natural oxidation reactions involving the exposed sulphides, water, air and microorganisms and is summarised by the following equations:



The release of deleterious metals under such acidic conditions has historically resulted in widespread environmental degradation with recent examples including Fly River, Papua New Guinea; Iron Mountain, California, USA; Kalgoorlie, Australia and Wheal Jane, UK [10, 16, 19 23]. Static and kinetic geochemical tests are commonly used to predict ARD generation. Static

tests involve determination of net-acid production potential (NAPP) and/or net acid generation (NAG) values (expressed in either kg H₂SO₄/t as used here or kg CaCO₃/t). NAPP is calculated through acid base accounting (ABA) procedures whereby the acid neutralising capacity (ANC) is subtracted from the maximum potential acidity (MPA). ANC determination involves the addition of acid (typically HCl) to a pulverised sample and back titrating the resulting liquor with NaOH following the Sobek Method or its derivatives [29]. MPA is calculated by multiplying the sulphur content by a stoichiometric factor. Positive NAPP values indicate a potential to generate acid. NAG values are obtained through the reaction of pulverised sample with H₂O₂ to accelerate sulphide oxidation with the resulting liquor titrated with NaOH and NAG (kg H₂SO₄/t) and NAGpH values calculated [26]. NAPP and NAGpH values are plotted graphically with samples classified as potentially acid forming (PAF), not acid forming (NAF) or uncertain (UC). Advanced static tests can be performed and include Kinetic NAG, Sequential NAG, Multi-Addition NAG and the Acid-Buffering Characteristic Curve (ABCC) tests; industry use of these tests is steadily growing [26, 27, 28]. Whilst static tests provide an indication of the potential to generate acid, there are many associated shortcomings [6, 16]. Kinetic tests better constrain the ARD generating potential by modelling the mine-environment through controlling variables such as temperature and humidity. These can involve either the construction of a field cell or laboratory bench scale tests [2, 8, 13, 16, 18, 24]. Whilst kinetic tests provide the most accurate predictions, they are time consuming (>30 weeks) and costly thus limiting their application.

Various attempts to directly predict ARD generation from mineralogy have been made over the past two decades as outlined in [17]. Blowes and Jambor [3] used pyrite-pyrrhotite bearing tailings samples to develop the Sulphide Alteration Index (SAI) which petrographically ranked the degree of weathering of sulphide grains (1-low, 10-high) and based on this assessed the remaining acid generating potential. This approach was also used by Shaw et al. [25] for pyrrhotite-pentlandite-bearing tailings samples. Most recently, application of QEMSCAN[®] [22] to assess ARD generating potential was presented in [9]. Other techniques used to predict ARD generation include calculation of neutralising potential (NP) directly from estimates based on whole-rock geochemical analysis and X-ray diffraction (XRD) which are discussed in [7, 14, 20, 21]. In the short-term a simple mineralogical screening method based on intact mineralogy is required. This method should be used in conjunction with traditional geochemical data to provide a more accurate ARD estimate. The development of one such potential method termed the ARD Index is described in this paper.

MATERIALS AND METHODS

Study Area

Three rock-piles (1-3) at an Au-mine site located in North Australia were sampled in this study. This mining operation has been abandoned since the late 1990s. The site is geologically classified as an orogenic lode-Au deposit, with the geology described as hydrothermally-altered felsic rhyolitic to rhyodacitic lavas, ignimbrites and tuffs. Gold and base-metal mineralisation is hosted by these felsic volcanics within metre-scale quartz reefs. Au-mineralisation is primarily associated with pyrite and arsenopyrite, with base-metal mineralisation associated with galena and sphalerite. These felsic volcanics have been subjected to varying degrees of alteration, from silicification, to replacement by sericite, and later alteration to clay (kaolinite). Sericite alteration is common in the wall rocks adjacent to Au-bearing quartz veins. Cretaceous conglomerates, sandstones, shales and siltstones unconformably overlie these felsic volcanics. No carbonate minerals have been identified in this area, thus an ARD problem exists.

Pile 1 is a low-grade ore stockpile (~0.5-1g/t Au) with localized ARD occurrences reported around the base. Pile 2 (the largest) contains a high proportion of sulphidic waste rock, with seepage from this pile measured between pH 3-4. The pH recorded from the surface of an

adjacent pit lake adjacent was acidic (pH 3.3) and significant elevations of heavy metals have also been recorded (including Cd, Pb, Zn and minor Cu). This pit-lake discharges into the local creek-system causing poor water quality for at least 40km downstream of the site. The third sampled waste-rock pile (pile 3) is located 4km to the east of the sites 1 and 2; ARD has not been reported to emanate from this site.

Sample Preparation

Fifty-one waste rock samples were collected to provide a range of lithologies from four different locations across the sites (suites C1WX from pile 1; C2WX& C3WX from pile 2; and CG1WX from pile 3). Identification of the alteration minerals present in hand specimen samples was performed using a portable-infrared mineral analyser (PIMA-II) spectrometer which essentially differentiated between pale-coloured alteration minerals (e.g. clays and micas) based on the short wave-infrared (SW-IR) absorption spectrum collected from a clean, dry flat, rock surface. Hand-specimen samples were cut in two, with the smaller piece polished for mesoscale texture classification. Sample areas were then selected for petrological and SEM analysis with polished thin sections made. The other sample portion was jaw crushed to <5cm, a split was taken and the remainder of material was ground in a ring mill to <125 μ m. Two sub-samples (each ~50g) were taken from each sample and used for acid-base-accounting (ABA) and net-acid-generation (NAG) testing.

Geochemical Characterisation

Static ABA tests were performed at both the Centre of Excellence in Ore Deposit Research (CODES), University of Tasmania and the Centre for Mined Land Rehabilitation (CMLR), University of Queensland. Static-tests were chosen based on suitability to the sample mineralogy. Tests were performed on all samples and included paste pH, Sobek, Modified Sobek and NAG tests following the procedures outlined in [29] and [1]. To deduce experimental error selected samples were tested in triplicate with reference samples KZK-1-376 and NBM-1 (obtained from CANMET) also tested, and as an extra measure randomly selected samples were sent to ALS Laboratories, Brisbane, Australia. Experimental error for NAG and acid neutralising capacity (ANC) tests performed at these different laboratories was calculated as <5%. Advanced geochemical tests such as the Sequential NAG and Multi-Addition NAG tests were performed on selected samples following procedures outlined in [26] and [29]. The bulk elemental composition of all samples was assessed by X-ray fluorescence (XRF) at the University of Tasmania using a Philips PW1480 X-ray spectrometer. Elemental Microanalysis (or EA) was also performed at the Central Science Laboratory, University of Tasmania using a Thermo Finnigan 1112 Series Flash Elemental Analyser. In this analysis 10mg of pulverised sample is placed in a tin capsule and heated to 900°C with spectra of sulphur, carbon, hydrogen and nitrogen gases evolved as SO₂, CO₂, H₂O and NO₃ measured and converted into wt. % of the sample. This analysis was performed to test its use as a low-cost method to quantify total-S content for calculating maximum potential acidity (MPA) values. These data were cross-checked with XRF total-S values to check the accuracy with <5% error calculated.

Mineralogical Characterisation

The hand-specimen samples were mineralogically grouped into ten categories which are here termed as 'mesotextures' (Figure 1). One representative sample was selected from each and a 3cm x 3cm area was classified by the ARD Index based on sulphide and alteration mineralogy using a binocular microscope and PIMA spectral data. A 'representative' polished thin section was then made and also classified by the ARD Index through reflected and transmitted light petrography and where appropriate internal sulphide morphology was examined using SEM images. ARD Index values obtained from both hand-specimen and thin section evaluations were averaged to obtain a final value as described in equation 1.

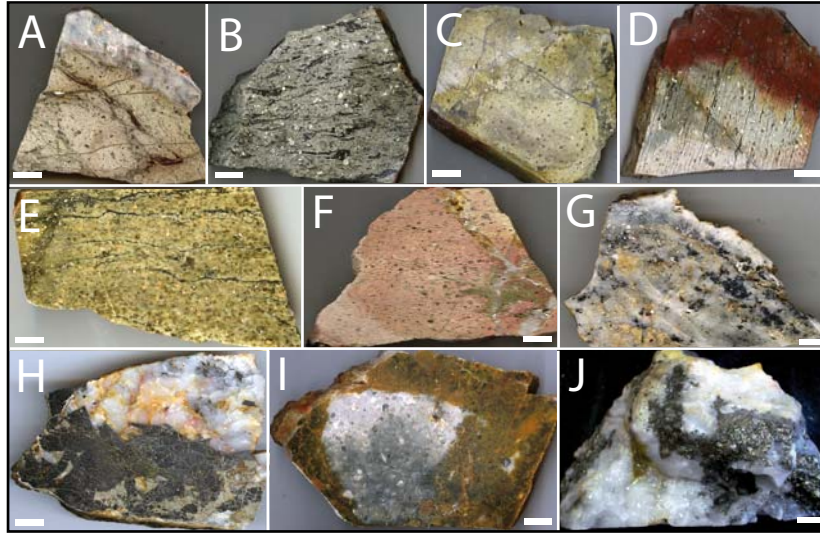


Figure 1: Representative mesotextures of the ten main lithologies sampled A-C1W5 B-C2W4 C-C2W5 D-C2W7 E-CG1W1 F-C2W8 G -CG1W2 H-CG1W8 I-CG1W9 and J-C2W13 (scale bar =1cm). NB. Description of mesotextures is given in Table 3.

The ARD Index evaluated each acid-generating sulphide-phase by five parameters: A- diameter/size of acid generating phase, B-degree of alteration of acid generating phase, C- morphology of acid generating phase, D-content of neutralising phases and E- spatial relationship between acid generating and neutralising phases. These parameters were chosen based on their direct control on ARD generation. Each category was ranked out of 10, summed and scored out of 50. Scores are averaged across the sample to given an overall score for the examined sample area. Equation 1 shows how final ARD Index values are derived following a staged evaluation.

Stage 1

$$\text{Me} = [A_{0-10} + B_{0-10} + C_{0-10} + D_{0-10} + E_{0-10}] = X$$

$$\frac{\sum X}{\text{No. of Me phases}} = X^1$$

Me = Mesoscale phase

Mi = Microscale phase

A = *Diameter/Size* of acid generating phase

B = *Alteration* of acid generating phase

C = *Morphology* of acid generating phase

D = *Content* of neutralising phases

E = *Spatial relationship* between acid generating and neutralising phases

Stage 2

$$\text{Mi} = [A_{0-10} + B_{0-10} + C_{0-10} + D_{0-10} + E_{0-10}] = Y$$

$$\frac{\sum Y}{\text{No. of Mi phases}} = Y^1$$

X or Y = Total Score (/50)

$\sum x$ or $\sum y$ = Total score for all phases

X^1 = total for Me sample

Y^1 = total for Mi sample

Stage 3

$$\frac{X^1 + Y^1}{2} = \text{ARD INDEX}$$

(1)

Table 1 shows the ARD Index value classification and interpretations for this particular sample suite. The ARD Index was calibrated with static geochemical data as shown in Table 2. Samples achieving 21-30 were considered as (weakly) PAF (potentially acid forming); 31-40 AF (acid-forming) and 41-50 extremely AF. Samples scoring ≤ 20 are considered to be NAF (not acid forming).

Table 1. ARD Index value classification and interpretation for these samples

ARD Index Value	Classification	Interpretation
≤50	<i>EXTREMELY AF</i>	>30% content of cm-scale unweathered acid generating phases. No primary or secondary neutralising mineral phases identified.
≤40	<i>AF</i>	>10% content of cm-scale acid generating phases <i>and/or</i> low (<10%) content of secondary neutralising minerals which may be in direct contact with these <i>and/or</i> no primary neutralising minerals identified.
≤30	<i>PAF</i>	<10% acid generating phases sub-cm scale phases present <i>and/or</i> moderate content (<40%) of secondary neutralising phases in direct contact with acid generating phases <i>and/or</i> low (<20%) content of primary neutralising minerals (not in direct contact with acid generating phases) identified.
≤20	<i>NAF</i>	<10% disseminated mm-scale acid generating phases encapsulated in slow weathering mineral phases <i>or</i> direct spatial contact with primary neutralising phases.
≤10	<i>NAF</i>	No acid generating phases present.

Samples were screened initially to identify end-members of each ARD Index parameter to aid criteria development for the scores 0-10. All acid-generating sulphide phases and the adjacent phases were examined and imaged. Samples which do not contain sulphide-phases automatically score 0 for the three parameters 1-3 which consider acid generation. Attention was instead focussed on the examination of neutralising phases, with samples scored based on the content and available specific surface area of primary (i.e. calcite, dolomite and siderite with neutralising potential (NP) values in the range of 864-1086 kgCaCO₃/t as stated in [12]) and secondary neutralising phases (i.e. olivine, serpentinite, anorthosite, and chlorite with NP values in the range of 6-38 kgCaCO₃/t also given in [12]). If neutralising phases are present in significant quantities and/or in direct contact with acid generating sulphides, then a low score is given. If an acid generating phase is encapsulated in a phase(s) with an NP value of ≤2 e.g. quartz, K-feldspar, muscovite, kaolinite or talc [12] then a low score is given. If the acid generating phase is present as an inclusion in another acid generating phase (e.g. pyrite inclusions in a chalcopyrite grain) or borders such, then a higher score is given. Examples of microscale evaluations are shown in Figure 2.

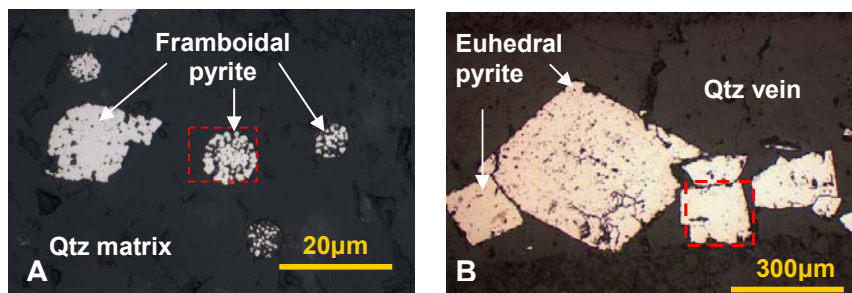


Figure 2: Microscale examples of ARD Index classification (reflected light images shown).

Photomicrograph A shows framboidal pyrite in a quartz matrix. The grain highlighted in the red box was evaluated by the five ARD Index parameters (/10): [1]1 (<20µm diameter); [2]2 (Fe-oxide coating the grain); [3]5 (framboidal with a relatively high specific surface area); [4] 10 (no neutralising minerals identified in field of view); [5]0 (contained in quartz). This scored 18/50 and is classified as NAF. Photomicrograph B shows pyrite grains contained in a fractured quartz vein and the highlighted grain evaluated (/10): [1]4 (<300µm diameter); [2]9 (coatings not identified, no internal fractures); [3]4 (euhedral grain with a relatively low specific surface area); [4]10 (no neutralising minerals identified in field of view); [5]6 (borders other euhedral pyrite grains but is contained in a quartz vein, which in turn is in a fine grained clay-matrix). This grain scored 33/50 and was classified as AF.

RESULTS AND DISCUSSION

Geochemical Classification

Given the low sulphate content of these samples (as evaluated from XRD, hand-specimen and petrological analysis), calculation of MPA directly from total-S was deemed appropriate, and was measured using EA and XRF. These two sets of data were in quantitative agreement ($R^2=0.98$), thus EA data was used in MPA and NAPP calculations. Samples demonstrating mesotexture J (Figure 1j) returned the greatest MPA values ranging from 140 to 520 $\text{kgH}_2\text{SO}_4/\text{t}$. Mesotexture H (Figure 1h) also returned an extremely high MPA value of 445 $\text{kgH}_2\text{SO}_4/\text{t}$.

Acid neutralising capacity (ANC) was calculated directly using both the Sobek and Modified Sobek methods. The Sobek method returned a range of -8.4 to 6.5 $\text{kgH}_2\text{SO}_4/\text{t}$ and the Modified Sobek returned a range of 19.8 -98.1 $\text{kgH}_2\text{SO}_4/\text{t}$. Based on the mineralogy of hand specimen samples (i.e. absence of carbonate minerals and low-content of longer-term neutralising minerals) it was concluded that the Modified Sobek Method has grossly overestimating the ANC by an order of magnitude as similarly found in [4] and [15]. The Sobek Method was thus concluded to be the most reliable for net-acid-producing-potential (NAPP) calculations for this particular suite of samples.

The single-addition NAG (herein referred to as NAG) test was performed on all samples and the results were compared with calculated NAPP values. An ARD geochemical plot of this data is shown in Figure 3. All samples demonstrating mesotextures J (massive quartz-pyrite with mm-scale Fe-oxide coating), G (massive quartz-veins with clotted sulphides dominated by sub-cm scale sphalerite and galena intergrowths) and H (massive quartz with cm-scale arsenopyrite-pyrite intergrowths and mm-scale disseminated galena) are classified as PAF; mesotextures B, D, F, I and A (with the one outlier) are NAF; and a spread is seen for mesotextures C and E which is likely due to the questionable reliability of using just 2.5g of powdered sample to define the ARD generating potential. Lithological descriptions of these mesotextures are given in Table 2.

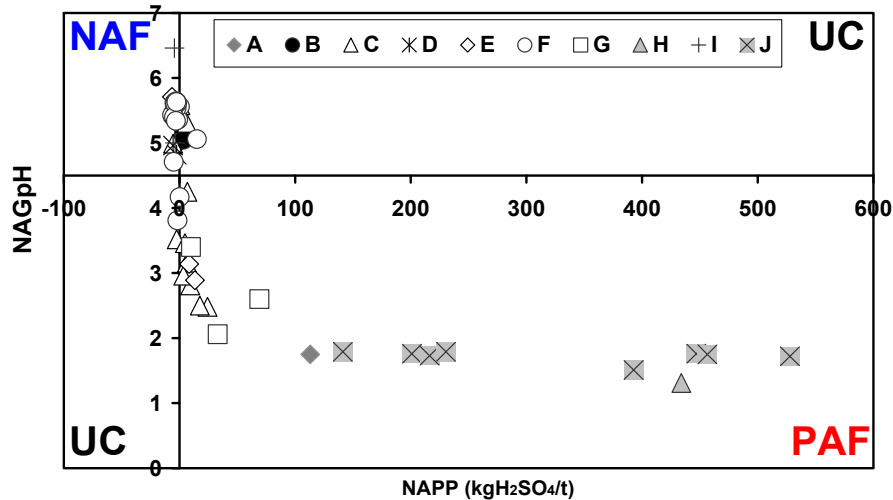


Figure 3: ARD Geochemical plot for all waste-rock samples grouped by mesotexture (PAF-potentially acid forming, NAF- Not Acid Forming, UC- Unclassified)

NAG tests generally returned lower values than NAPP ($R^2=0.73$). A series of advanced NAG tests were undertaken as recommended by Stewart (2005) and Weber et al., (2006) to check the accuracy of the NAG test. The sequential NAG (S-NAG) test was performed on five randomly selected samples (C1W3, C1W4, C1W10, C1W13 & C2W12). S-NAG results (to pH 7.0) were consistently higher than those returned by the NAG test. The greatest difference was recorded for sample C1W4 (mesotexture F), which by S-NAG returned a value of 29.9 $\text{kgH}_2\text{SO}_4/\text{t}$, and by NAG 1.0 $\text{kgH}_2\text{SO}_4/\text{t}$. The multi-addition NAG (M-NAG) test was also performed on these

samples. Sulphidic samples returned the least consistent results, with separate experiments showing sample C3W4 (mesotexture G) as NAF by the single-addition NAG test and PAF by the M-NAG test. This is likely because mesotexture G is polysulphidic, and thus the powdered sample used in each test may have contained varying proportions of the sulphides present (galena, sphalerite and minor pyrite). Despite this, these two remained the most consistent data sets in terms of quantitative agreement.

Comparing data from the four methods, the NAG test generally returned the lowest results likely reflecting incomplete sulphide oxidation (due to the denaturing of the 15% H₂O₂ used in the test) as detailed in [26]. NAPP values were the most erratic set of data returning the highest acid generating potential estimate for samples displaying mesotexture J (C1W3 and C1W13), and the lowest for samples displaying mesotexture F (C1W4). The S-NAG test generally returned the highest ARD generating potential results of the NAG tests. Comparing these results with total-S (wt. %) values obtained from EA it was decided that (single-addition) NAG values were adequate for calibrating ARD Index values for samples containing <0.5% S, and M-NAG values for samples containing >0.5% S.

Classification by the ARD Index

Representative polished slices and thin sections of each mesotexture were classified by the ARD Matrix with averaged values from meso- and microscale evaluation shown in Table 2. Based on the ARD Index mesotexture H and J were ranked the highest in terms of acid generating potential. This is in accordance with the M-NAG values calculated for these representative samples (446.1 and 433.1 kgH₂SO₄/t respectively). Mesotextures A, B, D, F and I were ranked as NAF (<10), which is in agreement with their NAG (<3.5 kgH₂SO₄/t), paste-pH (>4.5) and total-S (<0.3%) values. The ARD Index identified seemingly benign samples as represented by mesotexture E as (weakly) PAF; this is due to the presence of disseminated pyrite in a muscovite-kaolinite matrix thus weathering of these soft, fine-grained minerals is likely to occur at a greater rate than if contained in a quartz-matrix (e.g. mesotextural group B consisting of samples subjected to extensive silicification and classified as NAF). Mesotextures scoring <10 by the ARD Index have returned the highest Sobek ANC values, however the quantitative agreement between these data (R² = 0.57) suggests that improvements for assessing ANC are needed. Quantitative agreement between ARD Index values and (M)NAG geochemical results was sound (R²=0.85) as shown in figure 4.

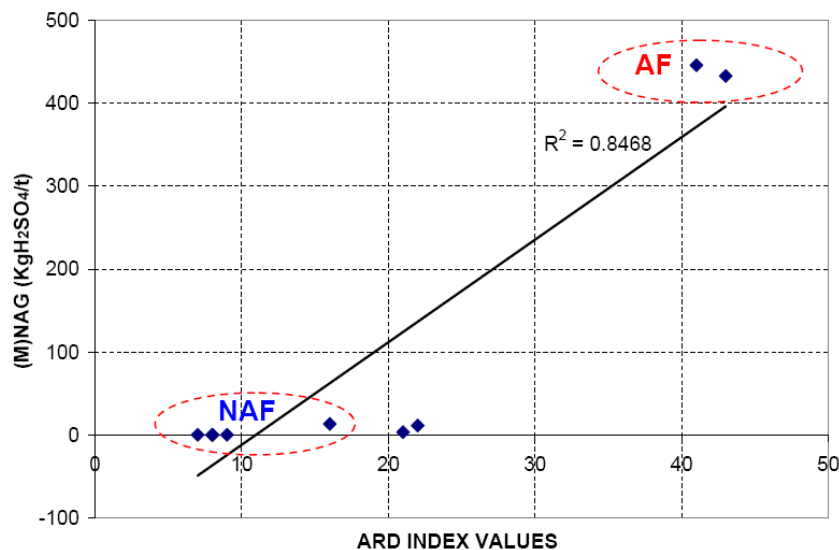


Figure 4: Correlation between ARD Index Values and (M)NAG geochemical results (AF- acid forming; NAF- not acid forming)

Table 2: Classification of mesotextures by ARD Index with geochemical data shown (rhy- rhyolite; qtz- quartz; fsp-feldspar; ill-illite; gph-graphite; gl-galena; py-pyrite; aspy-arsenopyrite; sph-sphalerite; mml-montmorillonite; msc-muscovite; chl-chlorite; kaol-kaolinite sc-sericite)

Meso-texture	Lithological description of mesotexture	Paste pH	Total -S (%)	Sobek ANC Value (Kg H ₂ SO ₄ /t)	(M)NAG (Kg H ₂ SO ₄ /t)	ARD Matrix (/50)	No. of samples
A <i>Fig 1a</i>	Pale-mid grey rhy with mm-scale qtz veins distributed randomly with sample bounded by larger >2cm barren qtz veins. Extensively kaolinitised, with sub-cm fsp phenocrysts altered to msc	6.86	0.27	4.35	0	8	3
B <i>Fig 1b</i>	Blue-grey silicified rhy with a 2mm Fe-oxide rind; mm-scale gph clots present. C.5% sub-rounded qtz phenocrysts	7.75	0.04	-1.90	0	7	4
C <i>Fig 1c</i>	Light-mid grey rhy-tuff, feldspathic groundmass extensively altered to msc, mm-scale disseminated py & c.5% qtz rounded phenocrysts	6.65	0.71	-2.40	13.10	16	10
D <i>Fig 1d</i>	Dark grey fine-grained banded rhy containing msc and ill. Mm-scale barren-qtz veins & gph 'blebs' round c.1mm (5%). Deeply weathered cm-scale red/brown Fe-oxide rinds	7.78	0	2.46	0	8	2
E <i>Fig 1e</i>	Felsic beige -grey coarse-grained banded rhy with a kaol and sc-dominated matrix and mm-disseminated py and a mm-scale weathering rind	4.74	0.26	-0.10	3.33	21	5
F <i>Fig 1f</i>	Mid-grey-pink fine grained rhy, extensive msc alteration with mm-qtz phenocrysts. Cm-scale barren qtz veining	8.4	0	2.54	0	8	13
G <i>Fig 1g</i>	Coarse qtz-vein with a 'honeycomb' texture, brittle with clotted sulphides dominated by >mm-scale sph (Cd-rich ZnS) and gl (PbS) intergrowths	5.38	2.25	-0.025	11.18	22	3
H <i>Fig 1h</i>	Massive qtz-sulphide with cm-scale aspy-py intergrowths and mm-scale disseminated gl (PbS)	5.05	14.30	-1.7	446.1	41	1
I <i>Fig 1i</i>	Highly weathered blue-grey porphyritic silicified rhy with a cm-scale rind altered to Fe-oxide, mml and chl	6.81	0.02	4.43	0	9	2
J <i>Fig 1j</i>	Massive qtz-pyrite with an mm-scale rind of Fe-oxide	1.72	16.62	-8.41	433.1	43	8

Whilst still requiring further technical development, the ARD Index presents a simple classification which could be undertaken as part of the 'Wheel Approach' (involving the use and cross-checking results from static ABA & NAG tests, field and lab-based kinetic tests, mineralogy, whole-rock data, retention tests and onsite monitoring) of [18]. Intended application at this abandoned mine operations (where deconstruction and redesign of the waste-rock piles has been proposed) would be domaining of waste-rock into these mesotextural groups and undertaking of detailed kinetic testwork.

ARD Generation at Waste-Rock Pile Sample Locations

The main lithologies found at each waste rock sampling location are summarised in Table 3. Samples collected from pile 1 (represented by suite C1WX) contained only two AF samples that

showed textural similarity to mesotexture J (cm-scale quartz-pyrite). Whilst the remaining fourteen samples collected from this site were classified as weakly PAF and NAF, these samples do not offer any effective neutralisation. An evaluation of the volume of each of these identified lithologies is required at this pile to establish the prevalence of mesotexture J, and estimate if significant ARD will eventually emanate from this pile. Samples collected from pile 2 (suites C2WX and C3WX) contained the most AF samples relative to the other piles; mesotexture J was again identified as the most prevalent ARD generating mesotexture and thus the likely source of ARD entering the local catchment. Based on the petrographic analysis of this mesotexture J, it was seen that (cm-scale) acid generating Fe-sulphides (dominantly pyrite) were relatively unaltered and thus represent a significant reservoir for long-term generation of ARD however current ARD generation is more likely to be controlled by finer-grained pyrite present detritally between individual waste-rocks. Pile 3 (represented by suite CG1WX), contained many waste rock boulders displaying mesotexture H (weathered sphalerite-galena-quartz (sphalerite was Cd-rich as confirmed by SEM-EDS and μ XRF). Site owners should focus attention on managing waste rock boulders demonstrating this mesotexture as these are the likely source of Cd. A reconnaissance survey is recommended to investigate the prevalence of these mesotextures and indeed to identify if any others exist.

Table 3: Frequency table of mesotextures sampled at each site (¹NAF ²weakly PAF, ³AF ⁴Extremely AF as per the ARD Index)

	A ¹	B ¹	C ¹	D ¹	E ²	F ¹	G ²	H ⁴	I ¹	J ⁴
Site 1: C1WX	3		2	1	4	3	1			2
Site 2: C2WX		4	6	1	3	1			1	4
Site 2: C3WX					2		1			3
Site 3: CG1WX			2		3	1	1	1	1	

Field Application of the ARD Index

Hughes [11] reported the use of paste pH and the carbonate-bomb test as ideally suited for rapid field characterisation. ARD Index assessment of mesoscale samples in the field could thus be complimentary to these tests. To explore this and understand the current ARD conditions, Index values were compared with paste-pH test values as shown in Figure 5. Samples with paste pH values of <4.5 have been classified as PAF in accordance with NAG pH V NAPP geochemical plots. Classifying samples in this manner (as opposed to a traditional ARD geochemical plot as shown in Figure 3) allowed each graphical field to provide a greater level of detail.

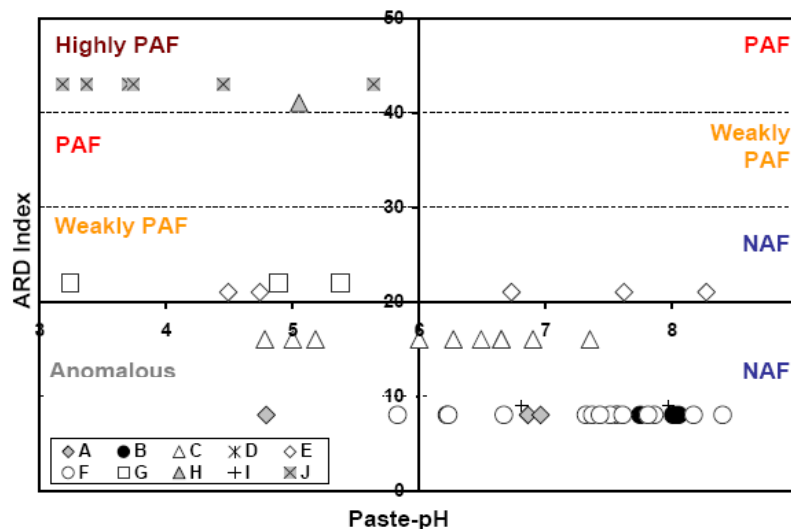


Figure 5: ARD Index Values of mesotextural groups compared with paste pH values

Samples demonstrating mesotexture J and H plotted mostly in the highly AF field. Mesotexture H returned a slightly lower paste-pH value than the majority of mesotexture J suggesting that arsenopyrite is less reactive in the paste-pH test than pyrite, which is representative of field-conditions as explained in [5] and thus should be considered when performing this evaluation. Mesotextures F and G are considered by this classification as NAF (with one exception containing <5% sub-cm pyrite), reflecting the dominance of non Fe-sulphides (i.e. galena and sphalerite) and/or acid-generating phases included in inert slow-weathering phases in these samples. These results are in agreement with static and advanced static test data for these samples. Based on this, there is a positive indication that the ARD Index could indeed be of use for assessing current ARD generating potential of rock samples. The ARD Index also shows potential application by applying the concept of mesotextural grouping and defining the ARD generating characteristics (using the mineralogical approach calibrated with geochemical data as applied here) when pit-wall mapping.

CONCLUSIONS

This investigation has shown the worth of characterising samples through assigning and populating mesotextural groups, and through detailed meso- and microtextural evaluation using the ARD Index, current ARD generation potential of units can be understood. The ARD Index builds upon the Sulphide Alteration Index as developed by Blowes and Jambor [3], and adds parameters which evaluate the content and context of acid generating and neutralising (both effective and long-term) phases present. Unlike geochemical tests, this mineralogical approach considers the state of intact sulphides rather than those pulverised (i.e. 100% liberated) as they are in geochemical ABA and NAG tests. Furthermore, geochemical tests typically utilise 2.5g of sample, which depending on the homogeneity of the powdered sample may not be representative of the modal mineralogy, thus leading to potential errors made when predicting ARD quantities. Despite shortcomings with static testing [6], calibration of the ARD Index was required. Preference was given to NAG tests for this, with the multi-NAG test favoured for samples containing >0.5% S to overcome the effects of hydrogen peroxide denaturing [26].

Comparison of ARD Index values with paste-pH values was performed to assess the use of the ARD Index as a field-based test and to deduce its ability to make a reasonable estimate of a rock-units current ARD generating potential. More detailed classification of samples was permitted in comparing these parameters than using traditional NAPP/NAG geochemical plots, with samples classified as Extremely PAF, PAF, Potentially PAF, NAF and Anomalous. Based on this, from the ten mesotextures identified from these fifty-one samples, only two (mesotexture H and J) are considered significantly acid-generating. This is important for mine-operators of this site in context of future management of these piles, as by visually identifying samples of these mesotextures, rapid domaining of the waste/stockpiled rock can be undertaken without the need for extensive ABA/NAG geochemical testing performed, and only systematic cross-checks made as per 'The Wheel Approach' [18].

Whilst the method presented here is a useful screening technique, to increase efficiency and accuracy automated ARD predictive mineralogical protocols are required. Advances made through the collaborative AMIRA P843 GEM^{III} project (JKMRC, University of Queensland, Australia and CODES, University of Tasmania, Australia) in the application of automated mineralogy platforms have founded the field of *geometallurgy*. Modifying these techniques and manipulating existing data-sets in order to predict the propensity of a rock unit to generate acid will be undertaken and cross-checked with geochemical data. The aim is to produce a time and cost-efficient automated predictive protocol to effectively predict acid generation. A novel '*Tiered Approach*' to ARD prediction is currently being developed and focuses on integrating the predictive geometturgical techniques developed in GEM^{III} with advanced and routine current ARD predictive tests.

ACKNOWLEDGEMENTS

The ARC Centre of Excellence in Ore Deposit Research (CODES) is acknowledged for funding this research project, as is the Society of Economic Geologists for provision of additional funds through a Graduate Student Fellowship Grant.

REFERENCES

- AMIRA P387A Prediction and Kinetic Control of Acid Mine Drainage: ARD Test Handbook**, (2002) [1]
- Bezaazoua, B., Bussieré, B., Dagenais, A.M., Archambault, M.** (2004). Kinetic Tests Comparison and Interpretation for Prediction of the Joutel Tailings Acid Generation Potential. *Environmental Geology*, 46, pp.1086-1101. [2]
- Blowes, D.W and Jambor, J.L.** (1990) The Pore-water Geochemistry and Mineralogy of the Vadose Zone of the Waite Amulet mine tailings impoundment, Noranda, Quebec. *Applied Geochemistry*, 5, pp. 327-346. [3]
- Capanema, L.X.L and Ciminelli, V.S.T.** (2003). An investigation of Acid Rock Drainage (ARD) Occurrence in a Gold Mine Located in a Southeastern Brazil Region. *Rev. Esc. Minas.* 56 (3), pp.201-206. [4]
- Craw, D., Falconer, D. and Youngson, J.H.** (2003). Environmental Arsenopyrite Stability and Dissolution: Theory, Experiment and Field Observations. *Chemical Geology*, 199 (1-2), pp. 71-82. [5]
- Dobos, S.K.** (2000). *Potential Problems with Geologically Uncontrolled Sampling and the Interpretation of Chemical Tests for Waste Characterisation and ARD Prediction.* 4th Australian ARD Workshop on Acid and Metalliferous Mine Drainage, Townsville, ACER, pp.25-29. [6]
- Downing, B.W. and Madeisky, H.E.** (1997). Lithogeochemical Methods for Acid Rock Drainage Studies and Prediction. *Exploration and Mining Geology*, 6 (4), pp.367-379. [7]
- Gilbert, S. E., Cooke, D. R. and Hollings, P.** (2003). The Effects of Hardpan Layers on the Water Chemistry from the Leaching of Pyrrhotite-Rich Tailings Material. *Environmental Geology*, 44, p. 687- 697. [8]
- Goodall, W.** (2008). *Automated Mineralogy in the Prediction of Acid Rock Drainage: Accessible Mineralogy using QEMSCAN®.* SME '08 26th February, 2008, Salt Lake City, Utah. [9]
- Hamilton, Q.U.I., Lamb, H.M, Hallett, C., and Proctor, J.A.** (1999) Passive Treatment Systems for the Remediation of Acid Mine Drainage at Wheal Jane, Cornwall. *Water and Environment Journal*, 13, pp. 93-103. [10]
- Hughes, J., Craw, D., Peake, B., Lindsay, P. and Weber, P.** (2007). Environmental Characterisation of Coal Mine Waste Rock in the Field: an Example from New Zealand. *Environmental Geology*, 53, pp. 1501-1509. [11]
- Jambor, J.L., Dutrizac, J.E. and Raudsepp, M.** 2007. Measured and Computed Neutralisation Potential from Static Tests of Diverse Rock Types. *Environmental Geology*, Issue 52, pp. 1019-1031. [12]
- Kargbo, D.M and He, J.** (2004). A Simple Accelerated Rock Weathering Method to Predict Acid Generation Kinetics. *Environmental Geology* 46, pp.775-783. [13]
- Lawrence, R.W and Scheske, M.** (1997) A Method to Calculate the Neutralising Potential of Mining Wastes. *Environmental Geology*, 32 pp.100-106 [14]
- Lawrence, R.W, and Wang, Y.** (1997). *Determination of Neutralisation Potential in the Prediction of Acid Rock Drainage.* 4th International Conference on Acid Rock Drainage, Vancouver, BC, pp.449-464. [15]
- Lei, L. and Watkins, R.** (2005). Acid Drainage Reassessment of Mining Tailings, Black Swan Nickel Mine, Kalgoorlie, Western Australia. *Applied Geochemistry*, 20 (3). pp. 661- 667. [16]

- Mills, C. and Robertson, A.** (1998). Acid Rock Drainage, EnviroMine. Retrieved November 12th 2008, from <http://www.technology.infomine.com/enviromine/ard/home.htm> [17]
- Morin, K.A, and Hutt, N.M.** (1998). *Kinetic Test and Risk Assessment for ARD*. 5th Annual B.C Metal leaching and ARD Workshop. Vancouver, Canada. [18]
- Nordstrom, D.K., Alpers, C., Ptacek, C.J. and Blowes, D.W.** (2000). Negative pH and Extremely Acidic Mine-Waters from Iron Mountain, California. *Environmental Science and Technology*, 34, pp. 254-258. [19]
- Paktunc, A.D.** (1999). Mineralogical Constraints on the Determination of Neutralisation Potential and Prediction of Acid Mine Drainage. *Environmental Geology*, 39 (2), pp.103-112 [20]
- Paktunc, A.D.** (2001) MODAN- A Computer Program for Estimating Mineral Quantities Based on Bulk Composition: Windows Version. *Computers and Geosciences*, 27, pp.883-886 [21]
- Pirrie, D., Butcher, A.R., Power, M.R., Gottlieb, P. and Miller, G.L.**(2004) *Rapid Quantitative Mineral and Phase Analysis using Automated Scanning Electron Microscopy (QEMSCAN)*. Potential Application in Forensic Geoscience. Geological Society, London Special Publications, 232, pp.123-136. [22]
- Salomons, W, and Eagle, A.M.** (1990). Hydrology, Sedimentology and the Fate and Distribution of Copper in Mine-Related Discharges in the Fly River System, Papua New Guinea. *Science of the Total Environment*, 97/98, p 315-334. [23]
- Sand, W., Jozsa, P.G., Kovacs, S.M., Sasaren, N., and Schippers, A.** (2007). Long-term Evaluation of Acid Rock Drainage Mitigation Measures in Large Lysimeters. *Journal of Geochemical Exploration*, 92 (2-3), pp. 205-211 [24]
- Shaw, S.C., Groat, L.A., Jambor, J.L., Blowes, D.W., Hanton-Fong, C.J. and Stuparyk, R.A.** (1998) Mineralogical Study of Base Metal Tailings with Various Sulphide Contents, Oxidized in Laboratory Columns and Field Lysimeters. *Environmental Geology*, 33 (1/2) pp.209-217.[25]
- Stewart, W.A.** (2005). Development of Acid Rock Drainage Prediction Methodologies for Coal Mine Wastes. PhD dissertation, University of South Australia. [26]
- Stewart, W.A., Miller, S.D. and Smart, R.** (2006). *Advances in acid rock drainage (ARD) characterisation of mine wastes*. Paper presented at the 7th International Conference on Acid Rock Drainage (ICARD), March 26-30, 2006, St. Louis MO. R.I. Barnhisel (ed.) Published by the American Society of Mining and Reclamation (ASMR), 3134 Montavesta Road, Lexington, KY 40502. [27]
- Weber, P.A., Hughes, J.B., Conner, L.B., Lindsay, P., and Smart, R.C. St.** (2006). *Short-term Acid Rock Drainage Characteristics Determined by Paste pH and Kinetic NAG Testing: Cypress Prospect, New Zealand*. Paper presented at the 7th International Conference on Acid Rock Drainage (ICARD), March 26-30, 2006, St. Louis MO. R.I. Barnhisel (ed.) Published by the American Society of Mining and Reclamation (ASMR), 3134 Montavesta Road, Lexington, KY 40502 pp.2289-2310. [28]
- White, W.W.III., Lapakko, K.A. and Cox, R.L.** (1999). *Static Test Methods Most Commonly used to Predict Acid Mine Drainage: Practical Guidelines for use and Interpretation*. The Environmental Geochemistry of Mineral Deposits Part A: Processes, Techniques, and Health Issues. Reviews of Economic Geology 6A, Plumlee, G.S. and Lodgson, M.J., (eds). pp. 325-338 [29]